Ultrafast dynamics of the lowest-lying neutral states in carbon dioxide

Travis W. Wright, Elio G. Champenois, James P. Cryan, Niranjan Shivaram, Chan-Shan Yang, and Ali Belkacem

Ultrafast Dynamics of the Lowest Lying Neutral States in Carbon Dioxide

Travis W. Wright,[1, 2] Elio G. Champenois,[1, 3] James P Cryan,[4]
Niranjan Shivaram,[1, *] Chan-Shan Yang,[1, 5] and Ali Belkacem[1]

[1] Chemical Sciences Division, Lawrence Berkeley National Laboratory, Berkeley, California 94720, USA
[2] Department of Chemistry, University of California, Davis, CA 95616, USA
[3] Graduate Group in Applied Sciences, University of California, Berkeley, CA 94720, USA
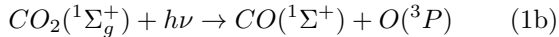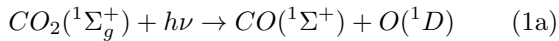[4] Stanford PULSE Institute, SLAC National Accelerator Laboratory, Menlo Park, CA 94025, USA
[5] Department of Physics, National Tsing Hua University, Hsinchu 30013, Taiwan

We present a study of the ultrafast dissociation dynamics of the lowest lying electronic excited states in CO_2 using ultraviolet (UV) and extreme-ultraviolet (XUV) pulses from high order harmonic generation. We observe two primary dissociation channels: a direct dissociation channel along the $^1\Pi_g$ electronically excited manifold, and a second channel which results from the mixing of electronic states. The direct dissociation channel is found to have a lifetime which is shorter than our experimental resolution, whereas the second channel has a significantly longer lifetime of nearly 200 fs. In this long-lived channel we observe a beating of the vibrational populations with a period of ~ 133 fs.

The interaction of carbon dioxide with vacuum ultraviolet (VUV) light is a fundamental process important to atmospheric and planetary chemistry. Carbon dioxide is the most abundant gas in the atmospheres of Mars and Venus and is the fourth most abundant on Earth [1]. The electronic excitations in carbon dioxide that are induced by the interaction with VUV light have been thoroughly identified through many spectroscopic experiments over the years [2–8]. High resolution absorption studies [7, 8] have identified two weakly absorbing valence states centered at 8.5 eV (146 nm) and 9.3 eV (131 nm) [8]. These two bands are traditionally identified as the $^1\Delta_u$ and $^1\Pi_g$ electronic states [9, 10].

It is well established that all the electronically excited valence states in CO_2 are predissociated [9, 11, 12]. The dissociation products of these valence states have been studied extensively and it has been found that there are two primary channels open, namely:

$$CO_2(^1\Sigma_g^+) + h\nu \rightarrow CO(^1\Sigma^+) + O(^1D) \qquad (1a)$$

$$CO_2(^1\Sigma_g^+) + h\nu \rightarrow CO(^1\Sigma^+) + O(^3P) \qquad (1b)$$

The ratio between these two channels depends on the excitation wavelength. For excitation wavelengths below 147 nm the $O(^1D)$ channel is dominant [13]. For excitation wavelengths above 147 nm the $O(^3P)$ channel dominates [14]. For wavelengths shorter than 147 nm it is likely that the molecule can directly dissociate on the initially-excited singlet manifold, where as for wavelengths longer than 147 nm there is likely a barrier to dissociation which allows for intersystem crossing via weak spin-orbit coupling resulting in triplet state dissociation. This has been verified by experiments performed at 157 nm where approximately 6% of the dissociation products are from triplet states [15].

In order to better understand the dissociation products and absorption spectrum of the lowest lying electronic states, considerable theoretical work has been performed modeling these states [9, 10, 16–18]. Most recently the active participation of the large number of degeneracies in this region has been carefully modeled to help explain spectroscopic features as well as the dissociation [19, 20]. These studies predict a large number of degeneracies between both the low-lying singlet and triplet states, and show that the $^1\Delta_u$ and $^1\Pi_g$ states cross within the Franck-Condon region leading to confusion on how to best label the features seen in experimental absorption studies [21].

Despite the large volume of experimental work identifying the dissociation products after excitation, there are relatively few time-resolved studies of these dissociation reactions. However, in the iso-electronic system CS_2, there have been many time-resolved experiments [22–24] and most of these works have focused on excitation near 200 nm which populates the $C^1\Sigma_u^+$ state of CS_2. The C-state will dissociate to produce $CS(X)+S(^1D,^3P)$. Previous experiments find two time-scales for the dissociation, a fast timescale which results from the direct dissociation of a slightly bent geometry [22], and a much longer time-scale (350 fs–650 fs) associated with dissociation along the $^1\Pi_g$ which is populated through a non-adiabatic transition as the molecule undergoes bending motion [22–24]. More recently, Spesyvtsev et al. employed higher time resolution to study the dynamics of the $^1B_2$ ($^1\Sigma_u^+$) state [25]. This work reveals a change in the electronic character of the excited state within a single vibrational period due to the mixing of nearby $^1\Pi_g$ and $^1\Delta_u$ states.

Due to the iso-electronic nature of CO_2, we expect to observe similar coupling dynamics when directly exciting the $^1\Pi_g$ state. Accessing these low lying neutral states of CO_2 requires 7 eV to 10 eV of photon energy. The difficulty in performing time-resolved experiments on CO_2 arises from the fact that none of these states are one photon dipole allowed from the ground state. Additionally, it is experimentally challenging to produce short, high flux

pulses of light in the 7 to 10 eV range. Here, we use a high flux high order harmonic generation source to excite CO_2 with two 4.77 eV photons and probe the dynamics with XUV photons.

To produce a high flux of XUV light, we use high order harmonic generation (HHG) in a loose focusing geometry [26]. A 1 kHz, 20 mJ, 25 fs, 780 nm near infrared (IR) Titanium doped Sapphire laser system is focused by a 6 m focal length focusing optic into a 10 cm gas cell containing 30 Torr of Argon gas. The pressure and location of the gas cell are optimized for production of the 3rd (260 nm, 4.77 eV) and 5th (157 nm, 7.95 eV) harmonics. Under these conditions the pulse energy of the 5th harmonic has been measured to be about 130 nJ (10^{11} photons/shot) using a calibrated photodiode while the pulse energy of the 3rd harmonic has been measured to be 5 μJ (6 x 10^{12} photons/shot). This configuration also gives a high flux of 11.1 eV (7th harmonic) and 14.3 eV (9th harmonic) photons, but minimizes the next possible photon energy at 17.5 eV and all orders above it due to reabsorption in Argon. The beam is back focused by a split mirror interferometer (SMI) [27] with two aluminum coated D shaped mirrors (f = 10 cm) into a velocity map imaging (VMI) spectrometer [28]. The 780 nm fundamental pulse is suppressed by four orders of magnitude using grazing incidence anti-reflection coated mirrors before the beam reaches the SMI. The pump arm is sent through a UV fused silica (UVFS) filter which removes the high orders and time separates the low orders since the different harmonics experience different group delays [29]. The pulse duration of the 3rd harmonic after passing through the UVFS filter was measured to be $\sim$ 20 fs using an autocorrelation measurement in Xenon. The probe arm consisting of 7th and 9th harmonics is sent directly to the back focusing mirror without any filters and their pulse duration is estimated to be $\sim$ 15 fs. The gas target is delivered to the interaction region through a 1 μm pinhole above the repeller plate. A more detailed description of our apparatus can be found in references [30, 31].

A graphical description of the excitation and probing scheme is shown in figure 1. Two 4.77 eV photons are used to excite the system to the dissociative $^1\Pi_g$ electronic state. The excited state dynamics of the molecule are probed by ionization with XUV radiation produced by HHG. This configuration gives a probe containing harmonics 3, 5, 7 and 9 including a weak fundamental at 1.59 eV.

Figure 2 shows the kinetic energy release (KER) of CO_2 as a function of pump-probe delay. At zero time-delay the 3rd harmonic in the pump arm overlaps with the probe arm creating a cross correlation feature. At probe early times, represented by negative time delays, the residual 780 nm IR light in the pump arm overlaps with the probe at around -200 fs since the UVFS imparts less group delay on the IR compared to the 3rd harmonic. At probe late times a time dependent effect can be seen extending for hundreds of femtoseconds up to a KER of
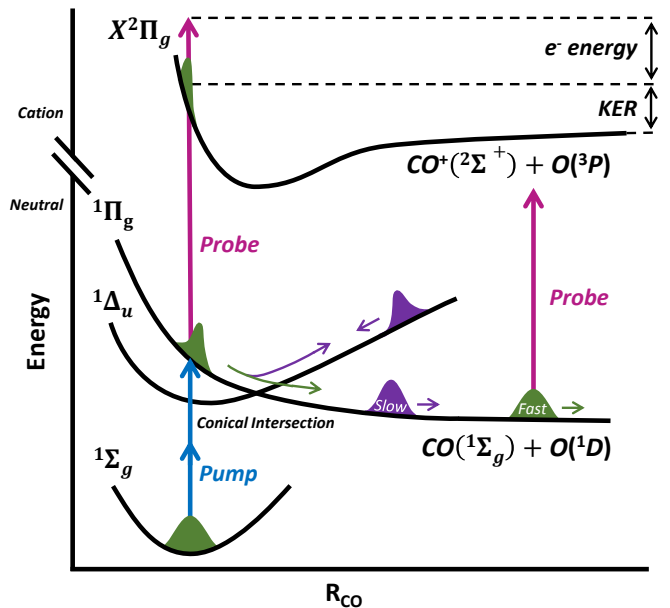

FIG. 1: A two photon pump (4.77 eV per photon - blue arrow) is used to excite the $^1\Pi_g$ state. As population on the $^1\Pi_g$ begins to dissociate a percentage of it transfers to other states through nonadiabatic transitions. These other states keep the molecule near the Franck-Condon region longer than is possible from the direct dissociation of the $^1\Pi_g$, allowing the probe (11.1 eV and 14.3 eV photons - magenta arrow) to generate more CO^+. Figure not to scale.

about 4 eV. The data in figure 2 is obtained by gating the detector for CO^+ and then scaling to obtain the values for the total KER. The angular distribution of the CO^+ fragment is isotropic due to the break-down of the axial recoil approximation and shows no variations as a function of pump-probe delay.

Creating CO^+ after excitation is only possible with either the 11.1 eV or 14.3 eV photons in the probe, simplifying the possible results. These photon energies can create CO^+ in two ways. The first is to ionize the excited CO_2 above a dissociation limit which is possible with both photon energies, and the second is to ionize the neutral dissociated CO which is only possible with the 14.3 eV photons since CO produced by dissociation of the neutral states exists in its ground electronic state and requires 14.0 eV to be ionized.

Having only two probe photon possibilities, the KER spectrum can be divided into two broad channels. Since excitation to the $^1\Pi_g$ involves the promotion of an electron to a $(1\pi_g)$ orbital, removing this electron would leave the molecule in the X state of the cation. The dissociation limit of the X state has been measured to be 5.69 eV above the X state or about 19.47 eV above the ground state of the molecule, and dissociates as $CO^+(X^2\Sigma^+)$ + $O(^3P)$ [32]. Two 4.77 eV photons followed by 11.1 eV gives 20.67 eV of total available energy leaving a little over 1.2 eV of energy available for kinetic energy release

(KER). Using 14.3 eV as the probe can give KER values as high as 4.37 eV. There are, therefore, two primary areas of interest: 0 to 1.2 eV of KER, and 1.2 to 4.37 eV of KER.

CO^+ ions with KER below 1.2 eV can have contributions from both the 11.1 eV and 14.3 eV probe photons. This region is represented by the green curve in figure 3 (a). Here a bi-exponential function provides a good fit to the data and exhibits two distinct lifetimes, one fast and one slow. Because the $^1\Pi_g$ drops by over 2 eV from the point of excitation and the 11.1 eV probe photons only have 1.2 eV of excess energy available for the dissociation, a window is set up in which the 11.1 eV photons can produce CO^+ in the cation. Using the approximate $^1\Pi_g$ curve provided in [33], we have performed a split operator propagation calculation for the wave packet on the excited state. This simple simulation, which considers only the asymmetric stretch coordinate, predicts that this window on the $^1\Pi_g$ is open for about 7 fs after excitation (time for 75% of the wave packet to clear the window). Direct dissociation along the $^1\Pi_g$ state as probed by the 11.1 eV photons is therefore likely responsible for the strong fast component of the bi-exponential as seen in figure 3 (a) in green. From the fit, we obtain a value of ~ 10 fs for the fast component of this 0 to 0.5 eV slice in figure 3 (a), which is shorter than our pulse duration.

Figure 3 (b) shows the lifetimes of the slow component of the bi-exponential decay as a function of KER. For the 11.1 eV probe, the slow decay represents a secondary population that can exist in the window longer than the direct dissociation would allow. Based on the ratios of
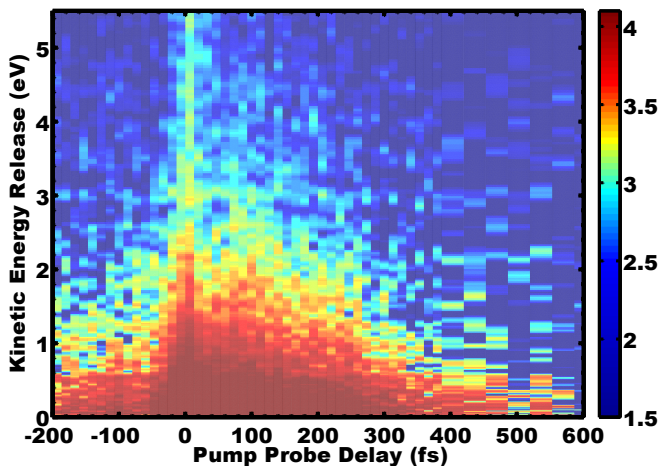

FIG. 2: Total kinetic energy release distribution as a function of pump-probe delay. The data plotted is CO^+, but the KER values are scaled to represent the total kinetic energy release of the molecule. Five probe early times (about 1 picosecond early) were averaged and subtracted through leaving only enhancements due to the pump-probe effect. The intensity is on a common logarithmic scale. Probe arrives early for negative time delays.
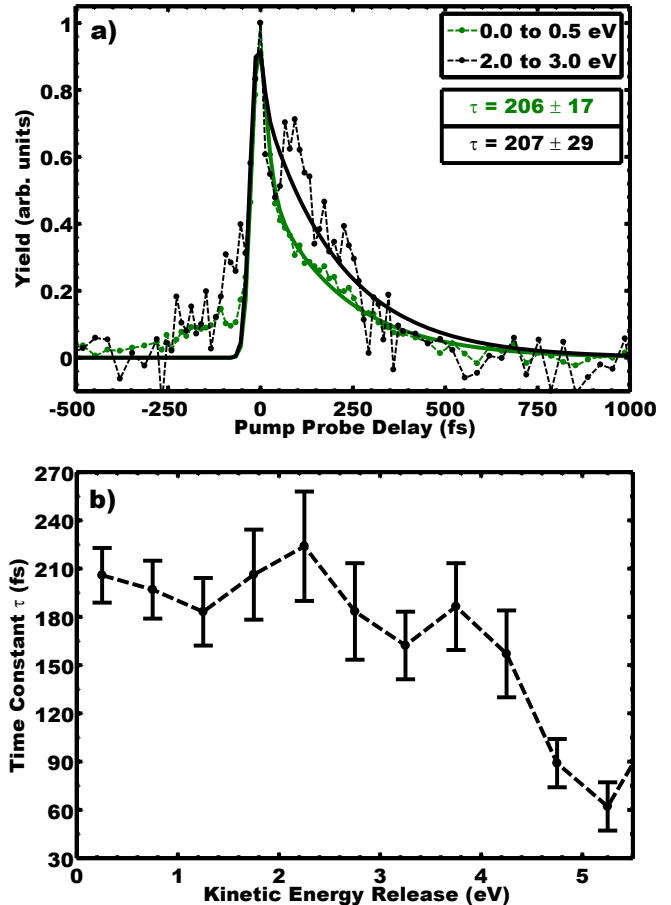

FIG. 3: a) Two KER slices of the distribution are taken and fit with a bi-exponential. The two slices are representative of the two KER regions - 0 to 1.2 eV and 1.2 eV to 4.37 eV - as discussed in the text. The data is scaled to have the same peak to probe late ratio, and then offset to have same probe late values in order to show shape differences. The quoted decay times are for the slow exponential. b) Many slices of the KER distribution. Same fit used as in a) with KER slices that are 0.5 eV wide and evenly spaced throughout the distribution, leaving no gaps. The slow decay times are plotted as a function of the center energy of the slice. The error bars represent absolute error obtained from the fit and increase (as a fraction of the time constant) at higher KER.

the exponential prefactors in the fit, this secondary population represents about 10% to 20% of the total. Theoretical work done by Grebenshchikov and Borrelli [34] predicts that a five fold degeneracy exists near linearity between the A' and A'' of the $^1\Pi_g$ and $^1\Delta_u$ states and the $^1\Sigma_u^-$. The schematic in figure 1 includes the $^1\Delta_u$ showing that in the stretch coordinate it is predicted to be a bound state. In the bend coordinate the $^1\Pi_g$ is stable while in the $^1\Delta_u$ the molecule is allowed to bend. Since the degeneracies described by Grebenshchikov are constrained to the linear geometry, it is feasible that transitions to the $^1\Delta_u$ would keep the probe window open
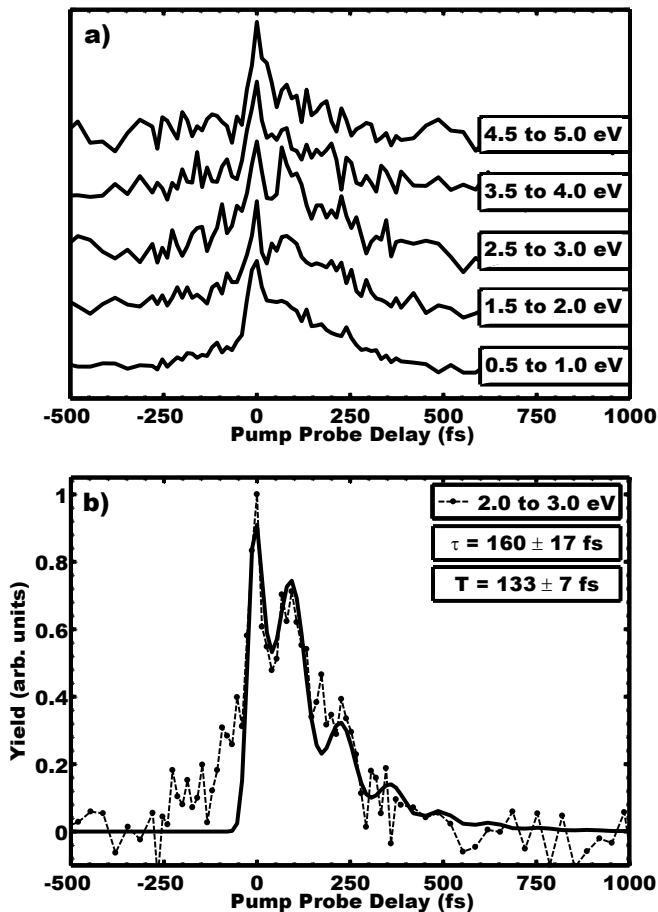
FIG. 4: (a) Five energy slices of the same size used in figure 3 (b) showing the deviation from a bi-exponential behavior. A clear secondary peak appears between 1.5 eV and 3 eV. (b) The same slice presented in figure 3 (a) in black but now fit with a single oscillating exponential instead of a bi-exponential. T is the period of the oscillations and τ is the exponential lifetime.

longer by allowing CO_2 to bend. This would delay transitions back into the $^1\Pi_g$ and explain the observed long time scale in the neutral dissociation. Recent work in CS_2 by Spesyvtsev et. al. [25] demonstrates that transitions similar to the one discussed here can occur within a single vibrational period. The two scenarios are not perfectly analogous, however, since in CS_2 the bound $^1\Sigma_u^+$ state is pumped as opposed to the dissociating $^1\Pi_g$ state in CO_2, but this does demonstrate that coupling occurs in the vicinity of the Franck-Condon region.

The experimental probe window with 11.1 eV photons can only contribute to data with a KER below about 1.2 eV. As seen in figure 2, there are still substantial counts above 1.2 eV representing 25% of the total observed CO^+ ions. Values of KER above 1.2 eV are dominated by contributions from the 14.3 eV photons. Even though 14.3 eV photons are not subject to a window effect, the long lifetimes in figure 3 are still too slow to be

from the direct dissociation of the $^1\Pi_g$ alone. Performing the same wavepacket propagation as before predicts that 75% of the population reaches an intermolecular separation of 5 bohr in the first 35 fs following excitation.

Extending from a KER of 1.2 eV to about 4 eV this subset of the signal exhibits a similar lifetime to that of KER below 1 eV (figure 3 (b)). However, as can be seen in figure 3 (a) in black, even though the fit lifetime remains similar, there is a qualitative difference in the shape of the decay. A bi-exponential in this region does not provide as good a fit as it did for values below 1.2 eV. Figure 4 (a) shows five slices centered on the most noticeable region of this deviation from the bi-exponential between 1.5 and 3 eV of KER. Figure 4 (b) shows a 1 eV slice from 2 to 3 eV which is the same as the black curve in figure 3 (a). Instead of being fit by a bi-exponential, figure 4 (b) shows a single exponential multiplied by an oscillating function. From the fit we obtain values of 160 fs and 133 fs for the exponential life-time and oscillation period respectively.

After excitation to the $^1\Pi_g$ state, the wave-packet moves towards the conical intersection between $^1\Pi_g$ and $^1\Delta_u$. In the vicinity of the conical intersection the wavepacket bifurcates and a fraction of the population dissociates on the lower $^1\Pi_g$ state due to the non-adiabatic coupling, as depicted in figure 1. The bound nature of the upper adiabatic surface means that the fraction of the wavepacket which remains on the upper state will eventually reach an outer turning point and reverse direction. This wave-packet will then revisit the vicinity of the conical intersection before returning to the Franck-Condon region. Depending on the anharmonicity of the upper state potential (which is small), the wave-packet on the upper state will continue its oscillatory motion, and each time it visits the conical intersection, a fraction of the population will transfer to the dissociative state. This coupling is similar to the coupling observed in reference [35], where oscillations with a period of 115 fs were observed, except in that experiment the two cationic states involved were both bound. Based on the spacings of the vibrational modes detected in spectroscopic studies such as reference [8], combinations of three or more such modes can lead to vibrational wave packet periods of over a hundred femtoseconds. Depending on which modes are activated in the accessible states, it is reasonable to have measured this relatively long period of 133 fs in our experiment.

In conclusion, we have performed a time resolved study of the lowest lying electronically excited states of carbon dioxide using UV and XUV photons to pump and probe the system. A two photon transition with a single photon energy of 4.77 eV was used to excite to the $^1\Pi_g$ state. After this excitation an XUV probe was used to produce CO^+ ions. This measurement reveals two primary channels. The first is the direct dissociation of the $^1\Pi_g$ state pumped by two 4.77 eV photons. We measured this to have a characteristic lifetime that is shorter than our time resolution. The second effect has a characteristic lifetime

measuring around 200 fs. By analogy to previous experiments performed in the isoelectronic molecule carbon disulfide, and from the theoretical predictions about the multiple degeneracies in the vicinity of the pumped state, we conclude that this long lived channel is the mixing of other states with the optically pumped state creating a delay in the dissociation. Within this long lived channel we additionally measure yield oscillations with a period of 133 fs on top of an exponential decay with lifetime of 160 fs when the CO^+ fragments are gated for higher kinetic energy release values. This possibly represents a revival period of wave packet dynamics on the excited state surface. Our measurement thus sheds light on ultrafast dynamics near this complex manifold of excited states in CO_2 which has not been previously explored experimentally.

[1] S. K. Bhattacharya, J. Savarino, and M. H. Thiemens, Geophysical Research Letters **27**, 1459 (2000).

[2] E. C. Inn, K. Watanabe, and M. Zelikoff, The Journal of Chemical Physics **21**, 1648 (1953).

[3] C. Cossart-Magos, S. Leach, M. Eidelsberg, F. Launay, and F. Rostas, Journal of the Chemical Society, Faraday Transactions 2: Molecular and Chemical Physics **78**, 1477 (1982).

[4] C. Cossart-Magos, M. Jungen, and F. Launay, Molecular Physics **61**, 1077 (1987).

[5] G. Stark, K. Yoshino, P. Smith, and K. Ito, Journal of Quantitative Spectroscopy and Radiative Transfer **103**, 67 (2007).

[6] R. I. Hall, A. Chutjian, and S. Trajmar, Journal of Physics B: Atomic and Molecular Physics **6**, L264 (1973).

[7] W. Chan, G. Cooper, and C. Brion, Chemical physics **178**, 401 (1993).

[8] K. Yoshino, J. Esmond, Y. Sun, W. Parkinson, K. Ito, and T. Matsui, Journal of Quantitative Spectroscopy and Radiative Transfer **55**, 53 (1996).

[9] P. J. Knowles, P. Rosmus, and H.-J. Werner, Chemical physics letters **146**, 230 (1988).

[10] A. Spielfiedel, N. Feautrier, C. Cossart-Magos, G. Chambaud, P. Rosmus, H.-J. Werner, and P. Botschwina, The Journal of chemical physics **97**, 8382 (1992).

[11] H. Okabe et al., *Photochemistry of small molecules*, vol. 431 (Wiley New York, 1978).

[12] Z. Chen, F. Liu, B. Jiang, X. Yang, and D. H. Parker, The Journal of Physical Chemistry Letters **1**, 1861 (2010).

[13] T. Slanger and G. Black, The Journal of Chemical Physics **68**, 1844 (1978).

[14] E. C. Inn and J. Heimerl, Journal of the Atmospheric Sciences **28**, 838 (1971).

[15] A. Stolow and Y. T. Lee, The Journal of chemical physics **98**, 2066 (1993).

[16] W. B. Englandb and W. C. Ermlerc, The Journal of Chemical Physics **70**, 1711 (1979).

[17] B. Zhou, C. Zhu, Z. Wen, Z. Jiang, J. Yu, Y.-P. Lee, and S. H. Lin, The Journal of chemical physics **139**, 154302 (2013).

[18] C. W. McCurdy Jr and V. McKoy, The Journal of Chemical Physics **61**, 2820 (1974).

[19] S. Y. Grebenshchikov, The Journal of chemical physics **138**, 224106 (2013).

[20] S. Y. Grebenshchikov, The Journal of chemical physics **138**, 224107 (2013).

[21] N. Watanabe, T. Hirayama, D. Suzuki, and M. Takahashi, The Journal of chemical physics **138**, 184311 (2013).

[22] D. Townsend, H. Satzger, T. Ejdrup, A. M. Lee, H. Stapelfeldt, and A. Stolow, The Journal of chemical physics **125**, 234302 (2006).

[23] C. Z. Bisgaard, O. J. Clarkin, G. Wu, A. M. Lee, O. Geßner, C. C. Hayden, and A. Stolow, Science **323**, 1464 (2009).

[24] P. Hockett, C. Z. Bisgaard, O. J. Clarkin, and A. Stolow, Nature Physics **7**, 612 (2011).

[25] R. Spesyvtsev, T. Horio, Y.-I. Suzuki, and T. Suzuki, The Journal of chemical physics **142**, 074308 (2015).

[26] T. K. Allison III (2010).

[27] T. Allison, T. Wright, A. Stooke, C. Khurmi, J. van Tilborg, Y. Liu, R. Falcone, and A. Belkacem, Optics letters **35**, 3664 (2010).

[28] A. T. Eppink and D. H. Parker, Review of Scientific Instruments **68**, 3477 (1997).

[29] T. K. Allison, J. van Tilborg, T. W. Wright, M. P. Hertlein, R. W. Falcone, and A. Belkacem, Optics express **17**, 8941 (2009).

[30] E. G. Champenois, N. H. Shivaram, T. W. Wright, C.-S. Yang, A. Belkacem, and J. P. Cryan, The Journal of Chemical Physics **144**, 014303 (2016).

[31] N. Shivaram, E. G. Champenois, J. P. Cryan, T. Wright, T. Wingard, and A. Belkacem, Applied Physics Letters **109**, 254101 (2016).

[32] Q. Meng, M.-B. Huang, and H.-B. Chang, The Journal of Physical Chemistry A **113**, 12825 (2009).

[33] S. Y. Grebenshchikov, The Journal of chemical physics **137**, 021101 (2012).

[34] S. Y. Grebenshchikov and R. Borrelli, The Journal of Physical Chemistry Letters **3**, 3223 (2012).

[35] H. Timmers, Z. Li, N. Shivaram, R. Santra, O. Vendrell, and A. Sandhu, Phys. Rev. Lett. **113**, 113003 (2014).